




Research Article

Spatio-statistical comparative approaches for landslide susceptibility modeling: case of Mae Phun, Uttaradit Province, Thailand



Muhammad Farhan UI Moazzam¹  · Anujit Vansarochana¹ · Jaruntorn Boonyanuphap¹ · Sittichai Choosumrong¹ · Ghani Rahman² · Geraud Poueme Djueyep³

Received: 24 November 2019 / Accepted: 23 January 2020 / Published online: 12 February 2020
© Springer Nature Switzerland AG 2020

Abstract

In this study for landslide susceptibility modeling, three quantitative techniques, i.e., frequency ratio (FR), information value (IFV), and weight of evidence (WOE), were evaluated and compared. For this purpose, landslide inventory map was prepared using visual interpretation on SPOT-5 image and field survey was carried out for ground truthing of landslide sites and total 677 landslides were identified. The inventory map was divided into training and validation datasets, and from total, 473 landslides (70%) were for training to run the model and 30% (204 landslides) for validation purpose. Total 11 landslide conditioning factors were used in this study that are: elevation, slope, aspect, curvature, plan curvature, profile curvature, land use/land cover (LULC), topographic wetness index (TWI), stream power index (SPI), proximity to road, and proximity to stream. Three different landslide susceptibility maps were produced based on analyzing the relationship of landslides with conditioning factors using FR, IFV, and WOE in GIS environment. The results of FR model indicated that almost 40% of the total study area fall in high to very high landslide susceptibility zones, while in WOE and IFV models, it was found almost 50% of the total area. The landslide susceptibility maps were validated using prediction and success rate curve techniques. The prediction rate curve gives us a glimpse of future landslides based on present landslide susceptibility maps. The results obtained from validation showed that the area under curve (AUC) based on prediction rate curve for FR, IFV, and WOE was 80.78%, 72.88%, and 72.33%, respectively. However, the AUC obtained through success rate curve for the models in this study was 74.60%, 75.04%, and 72.54% for FR, IFV, and WOE, respectively. Moreover, the evaluation of landslide density test and seed cell index area (SCAI) indicated that calculated and classified landslide susceptibility maps are in a good agreement with the field conditions. Thus, it was observed from this study that the frequency ratio has better accuracy as compared to information value and weight of evidence, but in success rate curve, almost all the models showed the same results. Consequently, it can be concluded that the susceptibility maps produced from FR, IFV, and WOE are in good agreement because more than two-third of landslides falls in high and very high susceptibility zones of each model. From this study, it was found that slope angle, elevation, land use/land cover, and roads play a major influencing role in the occurrence of landslide in the study area. The maps produced based on these landslide susceptibility models provide a base for engineers and land use planner to develop landslide management strategies before any development on slopes.

Keywords Frequency ratio · Information value · Weight of evidence · Landslide susceptibility · Prediction rate curve

✉ Muhammad Farhan UI Moazzam, farhan.moazzam@gmail.com; Anujit Vansarochana, anujitv@nu.ac.th; Jaruntorn Boonyanuphap, charuntornb@nu.ac.th; Sittichai Choosumrong, sittichaic@nu.ac.th; Ghani Rahman, ghani_geo@yahoo.com; Geraud Poueme Djueyep, pouemegeraud@gmail.com | ¹Department of Natural Resources and Environment, Faculty of Agriculture, Naresuan University, Phitsanulok, Thailand. ²Department of Geography, University of Gujrat, Gujrat, Pakistan. ³Department of Earth Sciences, Sapienza University of Rome, Rome, Italy.



SN Applied Sciences (2020) 2:384 | <https://doi.org/10.1007/s42452-020-2106-8>

1 Introduction

Landslides were found to be the most frequent and damaging natural hazard threatening human lives and properties [1]. Landslide is the devastating natural hazard causing serious human injuries, loss of lives, and heavy property damages every year in the mountainous region around the globe [2, 3]. The major triggering factors of landslides include earthquake, rainfall, storms, mining activities, and deforestation [4–6]. Every year thousands of people lost their lives, and about 4 billion dollars property damage occurs globally due to landslide [7, 8]. It is the third most devastating natural hazard in terms of damages after earthquake and flood [9]; however, individual landslide is not so obvious and devastating as an event of earthquake and flood [10]. Identification of the factors responsible for existing landslides is the initial step toward the prediction of future landslides by analyzing the most influencing factors, and the processes are known as landslide susceptibility mapping studied by various researchers around the globe [11]. Landslide is a natural phenomenon that cannot be completely stopped, but its associated risk can be minimized. Landslide susceptibility modeling identifies the vulnerable areas and its relationship with various influencing factors. Globally, it is a widely studied phenomenon and various quantitative and qualitative methods have been developed for landslide susceptibility modeling [10, 12]. The qualitative method helps to rank the conditioning factors based on the precedence scale, whereas the quantitative methods highly depend upon the relationship between conditioning factors and landslide inventory to classify the area into different landslide susceptible zones [13]. The researchers have used various models for landslide susceptibility mapping, i.e., analytical hierarchy process [14, 15], frequency ratio [8, 16, 17], information value [18, 19], weight of evidence [20, 21], and many other machine learning methods for landslide susceptibility assessment. In this study, three models IFV, WOE, and FR have been used as these three models are widely used in landslide studies across the globe and have been found most significant in landslide assessment in different mountainous regions of the world. The geographical information technology like GIS and remote sensing is widely used in the current century for such location-based issues like landslide hazard assessment [22]. In the past two decades, there has been an incredible transformation occurred in these technologies [23]. DEM is processed in GIS environment for the extraction of various thematic layers contributing toward the hazard assessment, i.e., elevation, slope,

aspect, curvature, topographic wetness index, and stream power index [24].

In the study area, rainfall and landslides have a direct relationship [25–27] and that is why in May 2006, heavy rainfall triggered a devastating landslide in Mae Phun, Thailand [28, 29], that caused 17 human losses and damaged 169 houses [29]. The main aim of this study is to compare three bivariate quantitative models, i.e., frequency ratio, information value, and weight of evidence model, and to suggest the most significant model for landslide susceptibility mapping in the study area.

Many studies have been conducted on landslides assessment and its effects in different parts of Thailand [30–34], although there is no such detailed study conducted on landslide for the given study area as well as in those studied they did not use that much detailed influencing factors for landslide modeling, which make this research different from the previous ones. For landslide prediction, it is assumed that the conditioning factors that caused landslide in past are responsible for initiation of landslide in future [7, 10].

2 Materials and methods

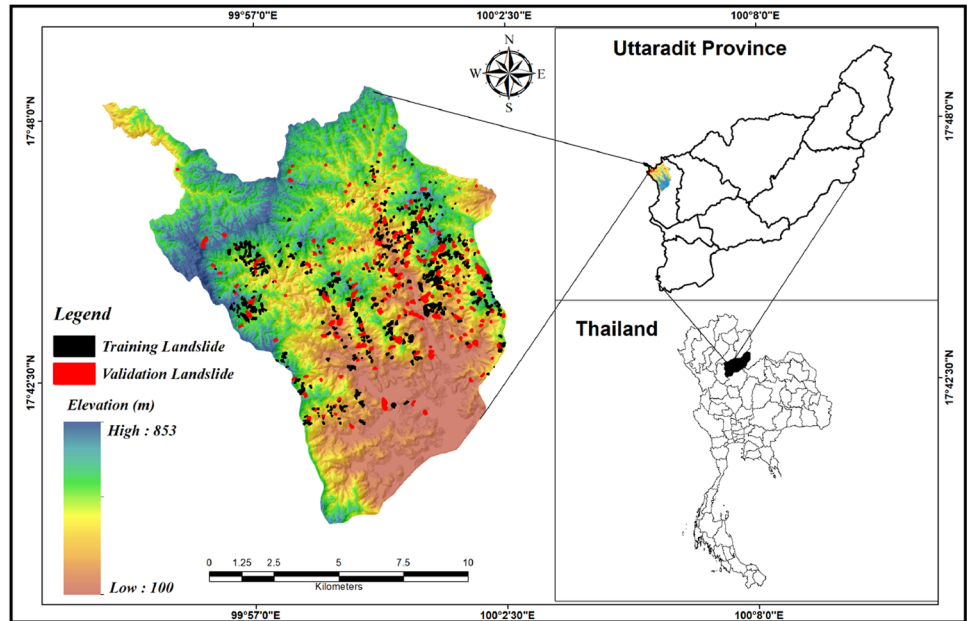
2.1 Study area

The study area is Mae Phun a sub-district of Laplae District, Uttaradit Province, that covers an area of 131 square kilometers. Elevation of the area varies from 100 to 853 m above mean sea level (Fig. 1). Slope gradient in the study area ranges from 0° to 69°. The area is located near the upstream of Nan river basin [28]. Most of the study area is covered with hillside and steep, narrow plain in valley groove [35]. The study area has tropical savanna type of climate, mean annual rainfall is 1506 mm, and mean annual humidity is 73% (1971–2010). In the months of May to October, monsoon brings heavy rainfall. Winter is dry and warm with an average maximum daily temperature 38.2° centigrade, and it rises in the month of April. The lithology of the study area consists of shale and siltstone in mountainous regions; however, alluvial deposits are present in the southern plain areas. Soil texture in the study area consists of mudstone, shale, and chest [28, 35]. Land cover in the study area consists of residential area, rural community, lowland paddy field, mountainous mixed deciduous upstream forest, and mixed fruit tree orchard in lowland areas [28].

2.2 Methodology

Landslide susceptibility analysis has four major steps: (1) collection and integration of data in spatial database, (2)

Fig. 1 Location map of the study area and landslide inventory



landslide susceptibility assessment using relationship of conditioning factors and landslide inventory, (3) validation of the results, and (4) comparison and interpretation of the results [36]. Figure 2 shows the detailed road map of this study.

2.3 Landslide inventory map

Mapping of past landslide area is an essential part of landslide susceptibility mapping [37]. In landslide inventory mapping, the information on past landslides location, type, time, depth of the landslides, etc., is collected [38]. Locations of past landslide were mapped

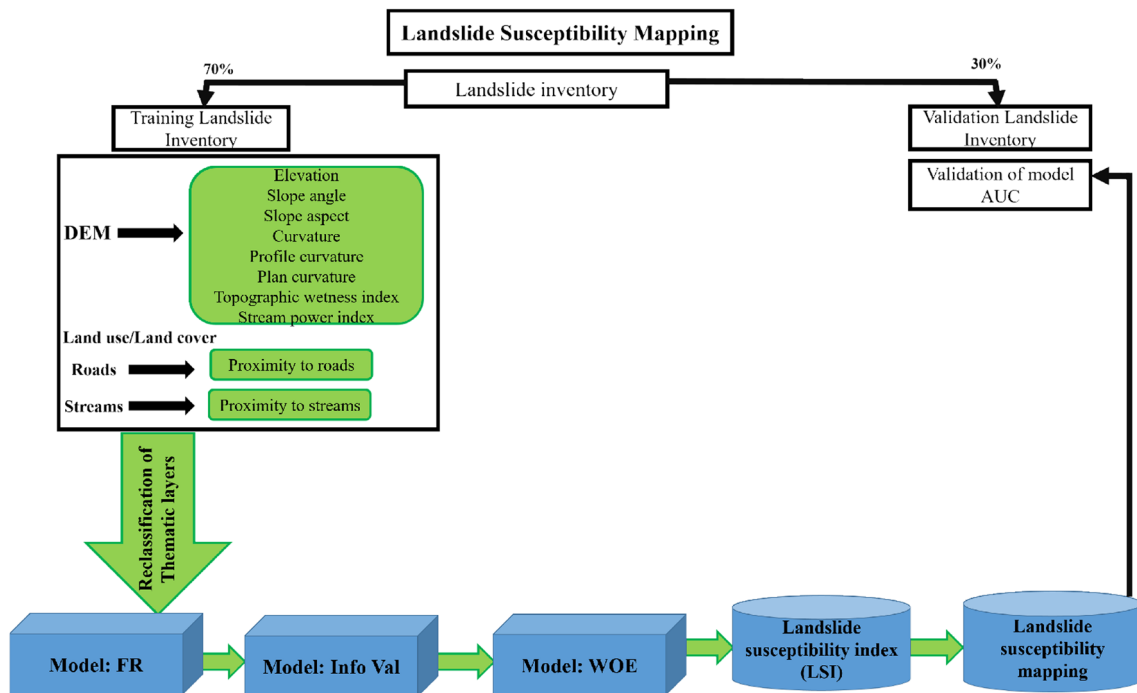


Fig. 2 Flowchart of research

on SPOT-5 image and then validated with field visits eventually, and 677 landslide locations were identified. Landslide inventory was drawn as a polygon layer in ArcGIS and then rasterized with 5 m × 5 m spatial resolution. Identified landslides cover an area of 4.25 km², which accounts 3.24% of the total study area. Landslide inventory data were randomly split into training and validation landslides as it is widely used percentages in the literature [39]; out of total, 473 (70%) were selected as training landslides (with an area of 2.68 km² accounting 2.04% of the total study area) to construct landslide susceptibility map, and the remaining 204 (30%) were used for validation of the applied models.

2.4 Landslide influencing parameters

Accuracy of the susceptibility map depends on the selection of the conditioning factors and assessment methodology [37, 40]. Although no specific guideline exists for the selection of the landslide conditioning factors [41], its selection depends on the nature of the study area and availability of data [42]. For this research, a thorough field study was carried out on the basis of field investigations, and literature reviewed helped to choose these 11 conditioning factors, i.e., elevation, slope, slope aspect, curvature, profile curvature, plan curvature, stream power index (SPI), topographic wetness index (TWI), land use/land cover, proximity to streams, and proximity to roads. Study area is affected by rainfall-triggered landslide that is why rainfall is considered as a triggering factor.

2.4.1 Land use/land cover

Many studies have shown strong relationship of land use with the occurrence of landslide [43–45], as barren land contributes more to landslide occurrence as compared to vegetative areas. The vegetative land reduces the impact of climate, and the roots bound the soil [18]. Deforestation, agricultural activities on slope, and construction of road network mostly disturb the slope stability and make it more susceptible to landslides [8, 46]. Clear-cutting of coppice for agricultural, buildings, or road development increases the risk of both landslides and floods [47]. Land use/land cover data were acquired from Land Development Department, Bangkok (Fig. 3).

2.4.2 Proximity to streams

It is a significant parameter for slope stability studies, and it can adversely affect the slope by vertical and lateral erosion and thus reduce the shear resistance [48, 49].

2.4.3 Proximity to roads

Roads are human-induced parameter which can cause landslide [41]. Extensive digging, extraneous loads, and deforestation are mostly observed near the road network, and all these support slope failure [1].

2.4.4 Rainfall

Rainfall is an extrinsic variable widely used in susceptibility analysis, and its spatial distribution of annual rainfall

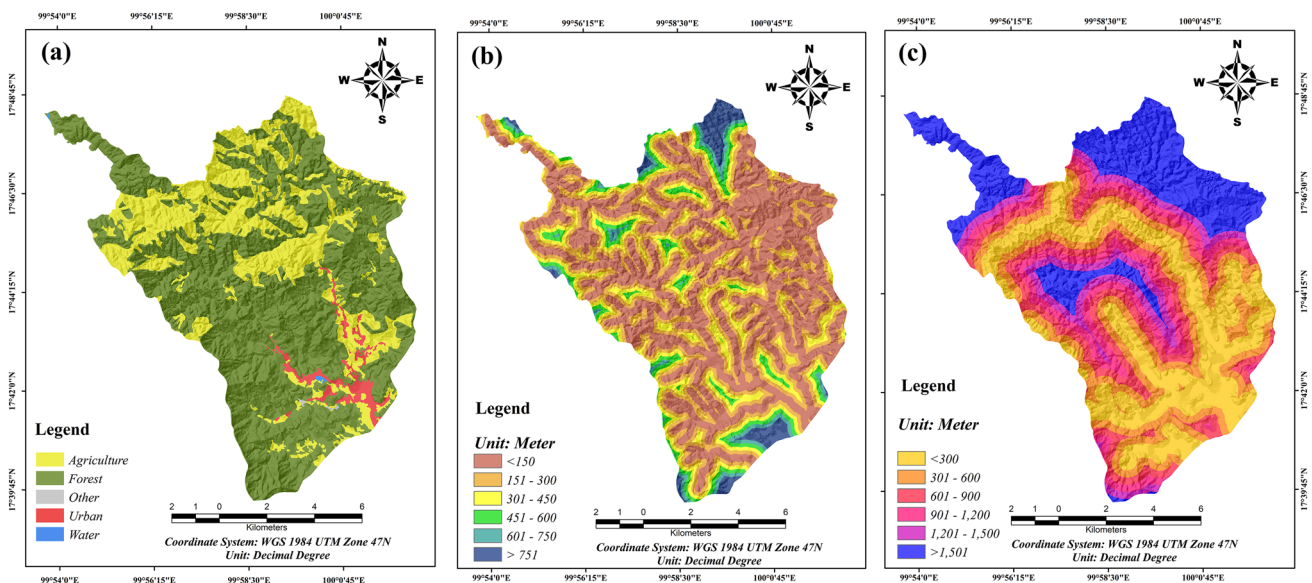


Fig. 3 a Land use/land cover, b proximity to streams, c proximity to roads

is commonly considered in statistical hazard analysis [50, 51]. In study area, landslide was triggered by heavy rainfall. Therefore, annual rainfall data of eight stations around the study area were used to prepare rainfall intensity map. Rainfall data were obtained from Thai Meteorological Department, Thailand. Rainfall intensity map was obtained by applying IDW technique (Fig. 4i). About 50% study area was dominated by two rainfall classes, i.e., 995.9–1037.8 and 1037.9–1068.6 mm/year.

2.4.5 DEM-derived conditioning factors

Digital elevation model data of the study area were downloaded from (Advanced Space borne Thermal Emission and Reflection Radiometer). All topographical parameters, i.e., elevation, slope gradient, slope aspect, slope curvature, plan and profile curvature, TWI, and SPI were extracted from DEM.

2.4.6 Elevation

It is considered as one of the important contributing factors in landslide occurrence [41, 52, 53]. It is an evident fact that the temperature decreases with elevation, while rainfall increases with increase in elevation. The high amount of rainfall on fragile slopes leads to landslide occurrence [44].

2.4.7 Slope gradient

It is another most widely used conditioning factor in landslide studies [3, 19, 41, 44], as it has a direct relationship with the occurrence of landsliding.

2.4.8 Slope aspect

It has relation with sunlight exposure, winds, soil moisture content on a slope, and these factors indirectly cause landslide occurrence [3, 10].

2.4.9 Slope curvature

It is an important geomorphic index of topographic feature, defined as the rate of change of slope in certain direction. It adversely affects the surface erosion by converging and diverging the runoff down the slope [54–56]. It has two utmost values: Positive values indicate the surface is convex in upward direction at certain location, while negative values specify that surface is concave in upward direction. Higher the negative value increase, the more the probability of landslide occurrence; on the contrary, comparatively flat area is less exposed to landslide. Slope with concave surface will tend to hold more rainfall water;

thus, it has more time for water infiltration into slope and thus increases the probability of landslide occurrence, but the case is opposite for convex slope [55].

The combination of *plan* and *profile* curvature along with curvature is taken into consideration so that slope morphology and flow can be better assessed.

2.4.10 Stream power index

SPI measures the erosive power of stream, and it is considered as a significant contributing factor that can control the slope stability in the certain area [57]. Higher SPI values indicate steep, straight, scoured reaches, and bedrocks; however, lower values represent broad alluvial flats, floodplains, and slowly subsiding areas, where the valley fill is mostly intact and deepening [58].

$$SPI = A_s \times \tan \beta \quad (1)$$

where “ A_s ” is the catchment area and β is the slope gradient in degrees.

2.4.11 Topographic wetness index

TWI is used to quantify the topographic control on hydrological process. TWI can measure the degree of accumulation of water at a site. TWI and landslide have a direct relationship if the value of TWI increases the occurrence of landslide [59]. TWI was extracted from DEM, and the formula is given below.

$$TWI = \ln (A_s / \tan \beta) \quad (2)$$

where “ A_s ” is the catchment area and β is the slope angle in degrees.

2.5 Frequency ratio model (FR)

FR is a bivariate geo-statistical method to compute the probabilistic correlation between independent and dependent variables [60]. For landslide prediction, it is assumed that the conditioning factors that caused landslide in past may be responsible for initiation landslide in future [7, 10]. The main advantage of FR model is that it is very easy to use and obtain the results that are readily intelligible [1].

FR is based on the correlation of landslides and its conditioning factors. FR is the ratio of the landslides to the total study area; in addition, it is also the ratio of landslide and non-landslide area for a given attribute/class of a parameter. Therefore, calculating FR values, the area ratio with landslide to non-landslide was computed for each class of each factor for the whole study area, and then, area ratio of each class of each factor to the whole study

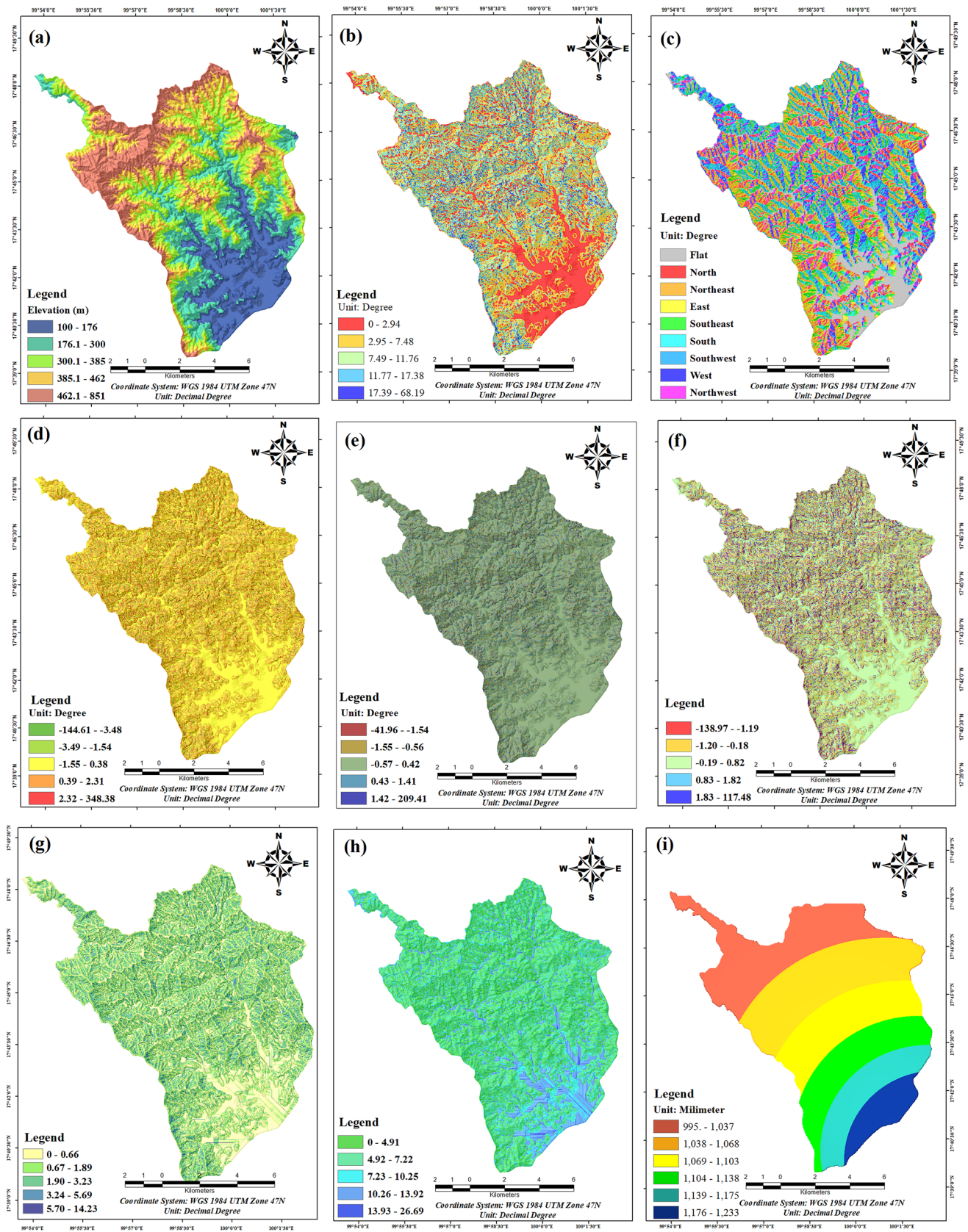


Fig. 4 a Elevation, b slope gradient, c slope aspect, d slope curvature, e plan curvature, f profile curvature, g stream power index, h topographic wetness index, i) rainfall intensity

area was calculated. Hence, FR value of each class type was obtained by dividing the ratio of landslide to the ratio of study area [1, 7, 21].

$$FR = \frac{N_{pix(Li)} / N_{pix(Ci)}}{\sum N_{pix(Li)} / \sum N_{pix(Ci)}} \tag{3}$$

where $N_{pix(Li)}$ is the landslide pixels in class i , whereas $N_{pix(Ci)}$ is the number of pixels in class i , $\sum N_{pix(Li)}$ is the total number of landslide pixels, and $\sum N_{pix(Ci)}$ is the total number of pixels in the study area.

To produce landslide susceptibility index (LSI), FR values of all the factors were summed up using Eq. 2. LSI map was classified into various classes based on landslide susceptibility.

$$LSI = \sum (Fr1 + Fr2 + Fr3 \dots Frn) \tag{4}$$

where LSI is the landslide susceptibility index; “Fr” is frequency ratio value of each conditioning factor, and “n” is the total number of factors used. The FR value of 1 (one) is normal; if the FR value is superior than 1(one), it means that the factor has high correlation with landslide and vice versa [1, 44].

2.6 Information value method (IFV)

The information value model was first developed by Yin and Yan [61] and later on modified by Van Westen [62]. This model is based on Bayesian algorithm [63]. It is a useful approach for landslide susceptibility mapping by determining the impact of parameters on landslide occurrence in the study area [64]. It can be used to estimate the information value for each class of a parameter by dividing the landslide density in each class to the total landslide density in the target area [62]. The main aim of the natural logarithm is to take into the consideration of large variation in the information values, and if the landslide density is lower than normal, it gives negative weights; on the contrary, it gives positive weights when the density of landslide is higher than average [65].

$$IFV = \ln \left(\frac{Densclass}{Densmap} \right) = \ln \frac{N_{pix(Li)} / N_{pix(Ci)}}{\sum_{i=1}^n N_{pix(L)} / N_{pix(C)}} \tag{5}$$

where IFV is the information value of each conditioning factor. Positive values of Li specify the relevant correlation of landslide incidence and its related conditioning factor; the higher the score is, the more stronger will be the relationship, and negative value indicates the inverse correlation of landslide and certain inducing factors [61]. Using Eq. 5, weight values for each class of the influencing parameter were calculated and landslide susceptibility

index (LSI) was prepared by summing up all the weight values of each factor using Eq. 4.

$$LSI = \sum_{i=1}^n IFV \tag{6}$$

where n is the number of influencing factors used, and IFV is the information value of each conditioning factor.

2.7 Weight of evidence (WOE)

WOE uses Naïve Bayesian approach to estimate the comparative significance by means of statistical values [32]. Initially, this method was used for identification of minerals [66] and later on used for landslide susceptibility assessment by many researchers [21, 50, 51].

Detailed mathematical formulation of WOE approach is given in [66], and weights of each landslide conditioning factor were calculated on the basis of the absence or presence of landslide in each class of conditioning factor.

$$P\left(\frac{A}{B}\right) = P\left(\frac{\left(\frac{B}{A}\right) \times P(A)}{P(B)}\right) \frac{P(A)}{P(B)} \tag{7}$$

In this approach, weights were computed for all the influencing parameters (B) and its relationship with the absence or presence of landslide (A) within the study area [66].

$$W+ = \log \left[\frac{P\{B/A\}}{P\{B/A^-\}} \right] \tag{8}$$

$$W- = \log \left[\frac{P\{B^-/A\}}{P\{B^-/A^-\}} \right] \tag{9}$$

where P is the probability, \log is the natural logarithm, B is the presence of desired class of landslide conditioning factor, \bar{B} is the absence of desired class of landslide conditioning factor, and A is the presence and \bar{A} is the absence of landslides. Positive ($W+$) indicates the positive relationship between the presence of landslide and given class of a conditioning factor and vice versa. Eventually, the difference between two weights is calculated using Eq. 10 which is known as the contrast weight. Based on contrast values, the spatial correlation of landslide and its influencing parameters can be described [21, 66].

$$W+ = \log[(LS_{in}\%)/(nonLS_{in}\%)] \tag{10}$$

$$W- = \log[(LS_{out}\%)/(nonLS_{out}\%)] \tag{11}$$

where $(LS_{in}\%)$ and $(nonLS_{in}\%)$ are the percentages of the presence and absence of landslide pixels in the given class

of a parameter, respectively, and $(LS_{out}\%)$ and $(nonLS_{out}\%)$ are the percentages of landslide and non-landslide pixels out of the desired class.

$$W^c = W^+ - (W^-) \tag{12}$$

Value of 'C' ranges from 0 to 2, whenever the value of 'C' tends to zero in any parameter, meaning that it does not have any impact on the distribution of landslide in the area; on the other hand, if the value is 2 or more, the relationship between the parameter and landslide is very strong.

3 Results and discussion

The landslide susceptibility maps were produced with three bivariate quantitative statistical models using GIS-based approach and compared with each other.

3.1 Frequency ratio and landslide susceptibility

The resultant FR values of each thematic layer are given in Fig. 5. The slope aspect results show that the north-east-, east-, southeast-, south-, and south-facing slopes have greater than 1 (one) frequency ratio value indicating high probability of landslide incidence in these classes of aspect map. Analyzing the relation of landslides with elevation, it was found that in the classes ranging from 177 to 462 meters, the value of frequency ratio is higher than 1 (one) and the other classes have less than one FR value. All the classes in degree slope map show strong relationship with land sliding as the value of FR is higher than one in all the classes except $0^\circ-2.94^\circ$ class. FR values for land use/land cover are higher only in the class of forest cover ($FR = 1.20$). The relationship between landslide and roads shows that the FR value ranges from 1.40 to 1.58 in 600–1500 m proximity to roads. The FR values for the relationship between streams and landslide are higher than 1 at the buffer classes, ranging from 151 to 450 m from the

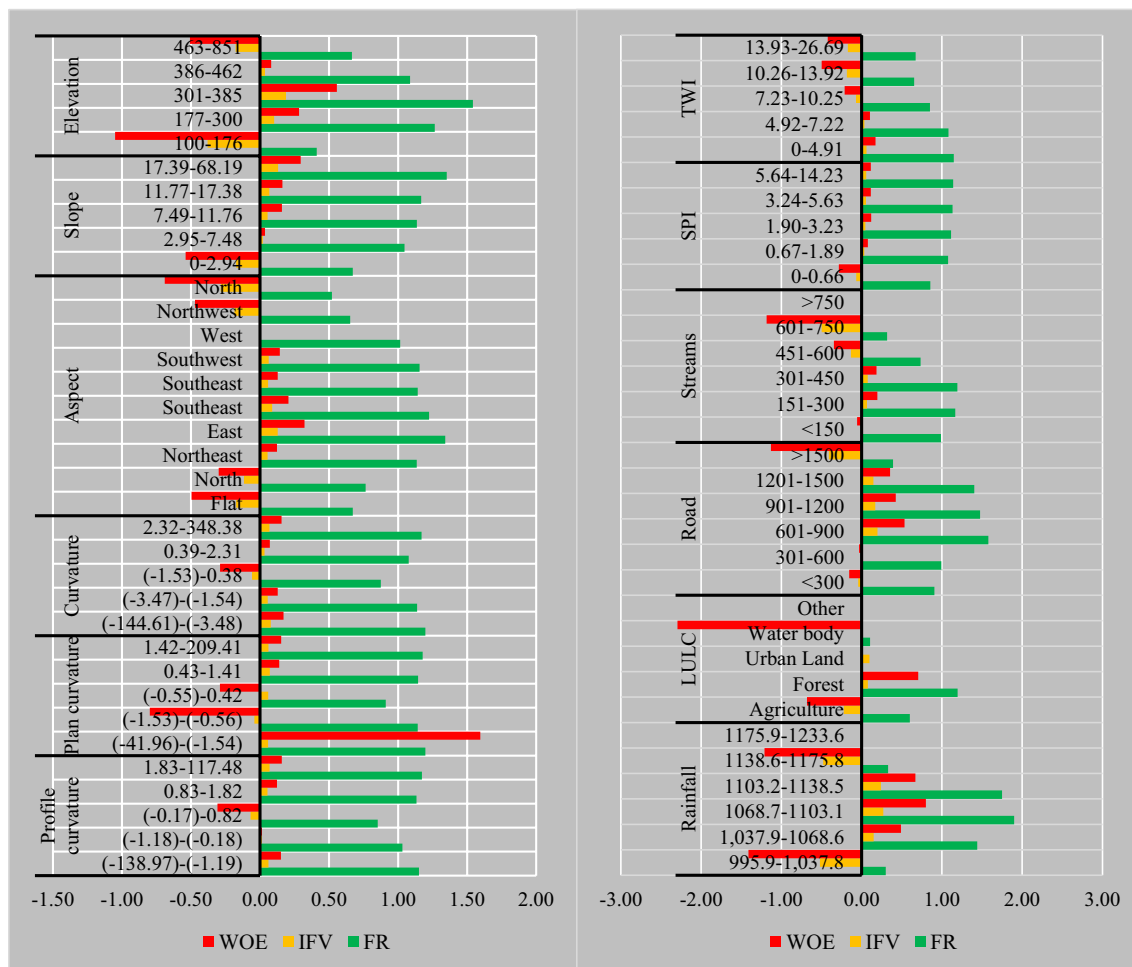


Fig. 5 Data used in the analysis and results obtained from frequency ratio, weight of evidence, and information value methods

streams. FR values were high for the TWI classes 0–4.91 and 4.92–7.22. The values of FR for SPI were 1.11–1.14 for the classes 1.90–3.23, 3.24–5.63, and 5.64–14.23, respectively. Curvature values indicate the morphology of the topography; positive values show upward convex, and on the contrary, negative values are showing upwardly concave surfaces. In curvature, both the concave area and convex area have higher FR values (1.03–1.20) that indicate higher possibility of landslide occurrence for all types of curvature. Resultant LSI map was reclassified into five various susceptibility zones ranging from very high to very low, classified with natural break method (Fig. 6a).

3.2 Information value and landslide susceptibility

To analyze the role of each class of a particular conditional parameter, the information value method was applied and the resultant weight was calculated (Fig. 5). Land use/land cover maps show that three-fourth of landslides occurred in the classes of forest and urban land having information value of 0.078 and 0.097, respectively, and agriculture land has lowest impact on landslide incidence (–0.222 information value). Slope is a significant and most widely used influencing factor and has been used by many researchers in landslide studies. It has a direct relationship with landslide, and analyzing the slope and landslide occurrence, the result shows that high landslide occurrence ranges from 2.95° to 68.19° slope classes, while the information value was minimum (–0.173) for the class of 0°–2.94°

slope. The result of information values for elevation and aspect ranges from –0.387 to 0.188 and –0.173 to 0.128, respectively, with approximately 79% of landslide area in the range of 177 m–462 m of elevation classes, and around 77% of landslide area is in the categories of NE-, E-, SE-, S-, SW-, and W-facing slopes of aspect parameter. As for TWI parameter, two-third of (76.52%) of the landslide incidences was found within the classes of 0–4.91 and 4.92–7.22, respectively. The concave and convex slope categories of curvature, profile, and plan curvature parameters have the highest information value, and the landslide area occupied by these categories is 56.54%, 61.74%, and 42.30%, respectively. As for distance from roads, highest information values were found within 600–1500 m around the road with information values ranging from 0.147 to 0.198. Distance from streams gives highest information value of 0.076 for the distance between 300 and 600 m followed by the class of 150–300 m with information value of 0.067.

LSI obtained from information value method was divided into five susceptibility zones and is shown in Fig. 6b.

3.3 Weight of evidence and landslide susceptibility

The positive and negative weights along with contrast values for each class of conditioning parameters are given in Fig. 5. The elevation class below 176 m and above 462 m

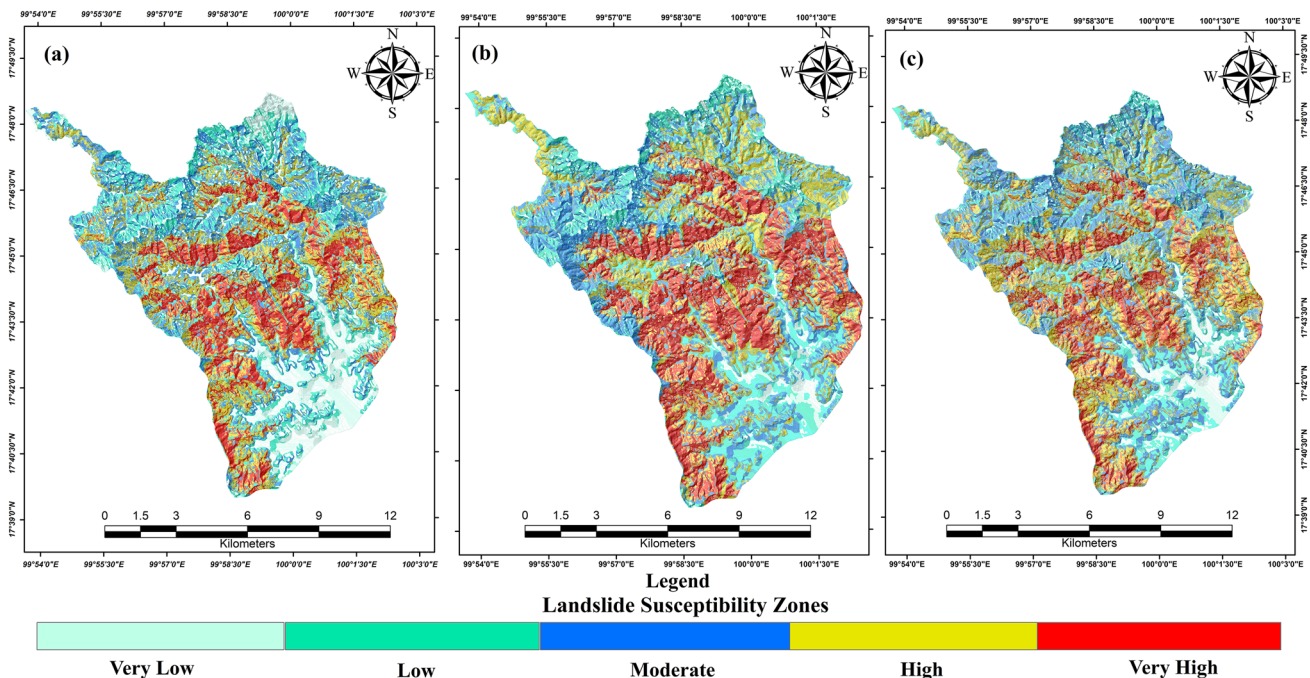


Fig. 6 Landslide susceptibility maps, **a** frequency ratio, **b** information value, **c** weight of evidence

showed higher correlation with landslide occurrence as the W^c value was found high.

Slope degree shows high tendency toward occurrence of landslides, as it is clear from the results of weight of evidence that all slope classes have higher contrast value except 0° – 2.94° ; as the slope gradient increases shear stress in soil, other materials also increase. As far as slope aspect is concerned, many landslides occurred on NE-, E-, SE-, S-, and SW-facing slopes with landslide area of 13.34, 16.84, 11.91, 12.06, and 13.11%, respectively. Results for land use/land cover map revealed that forest group has the highest W^c value of 0.71 with landslide area of 83.08%. In case of distance from the streams, the classes 151–300 and 301–450 m have positive correlation with landslide with values of W^c 0.20 and 0.19, respectively. Though, distance from the roads showed that the classes 601–900, 901–1200, and 1201–1500 meters has higher relationship with landslides, and area of landslide and contrast (C) values are 22.21%, 0.53, 15.54%, 0.42, and 11.42, 0.35, respectively. From these observations, it is elucidated that road construction is the most significant factor in slope failure. In TWI, classes 0–4.91 and 4.92–7.22 have the contrast value of 0.17 and 0.10, respectively, with landslide area of 32.74% and 43.78%, respectively, but in SPI, classes of 0.67–1.89, 1.90–3.23, 3.24–5.63, and 5.64–14.23 have the highest probability of landslide. Upwardly, concave and convex slope of curvature, plan, and profile curvature has positive relationship with landslides.

LSI map obtained from WOE model was classified into five susceptibility zones and is shown in Fig. 6c.

3.4 Validation of the models

All the three models were validated using prediction rate curves and success rate curves. Area under curve signifies the reliability of the model to predict the landslide events [67].

The validation landslides (30% of the total landslides) were used for predication curve, to predict the future landslides based on the present ones. The prediction rate curves were produced, and the area under curve (AUC) was obtained by plotting the landslides cumulative percentage area on y-axis against the cumulative percentage of landslide susceptibility area on x-axis. Success rate curve and prediction rate curve explain how well the model performed with the causative factor to predict landslides in future based on past landslides.

For success rate and predication rate curve calculation, landslide susceptibility index (LSI) values were divided into 100 equal classes which were sorted into descending order from very high to very low susceptibility classes. The validation and training landslide events were draped on

it, and the area under curve was calculated using zonal statistics tool in ArcGIS.

Results were obtained for success rate curve by relating the training landslides with landslide susceptibility index (Fig. 8). The success of the models showed the area under curve (AUC) 74.60%, 75.04%, and 72.54% for FR, IFV, and WOE, respectively.

Area under curve (AUC) value for the prediction rate curves of FR, IFV, and WOE was found 80.58%, 72.80%, and 72.33%, respectively (Fig. 7a). Thus, the AUC value for frequency ratio showed the highest accuracy in prediction rate curve, as compared to information value and weight of evidence. However, in success rate curve, almost all models showed the same accuracy. Frequency ratio and information value method showed almost same accuracy for success rate curve, but in prediction rate curve, the information value has better accuracy than frequency ratio for landslide susceptibility mapping in the study area. In this study, WOE model appears to be most reliable, since it corresponds close to the prediction of landslide potential in the study area.

3.4.1 Landslide density

An additional, landslide density test was also performed for consistency and quality of the landslide susceptibility models. Landslide density method was carried out on landslide susceptibility zones and validation landslide events. Landslide pixels were overlaid on susceptibility zones, and the density was estimated for landslide susceptibility zones. Landslide density values should increase with increase in susceptibility class [39]. In Fig. 7b–d, the bar graph shows the increasing trend of landslides with increment in susceptibility zones from very low to very high. Density of landslides slowly decreased from very high to very low landslide susceptibility zones. More than two-third of the landslides fall in high and very high susceptibility classes of all the models.

3.4.2 Seed cell index area (SCAI)

Seed cell area index (SCAI) used to test the accuracy of landslide susceptibility maps produced from FR, IFV, and WOE. SCAI was used on the classified landslide susceptibility maps and training landslides [68].

$$\text{SCAI} = \frac{\text{Landslide susceptibility zone (\%)}}{\text{Landslides in each susceptibility zone (\%)}}$$

It was assumed that the percentage of SCAI would be inversely proportional to the percentage of susceptibility zones [68]. Outcomes of SCAI obtained for all three approaches are shown in Table 1.

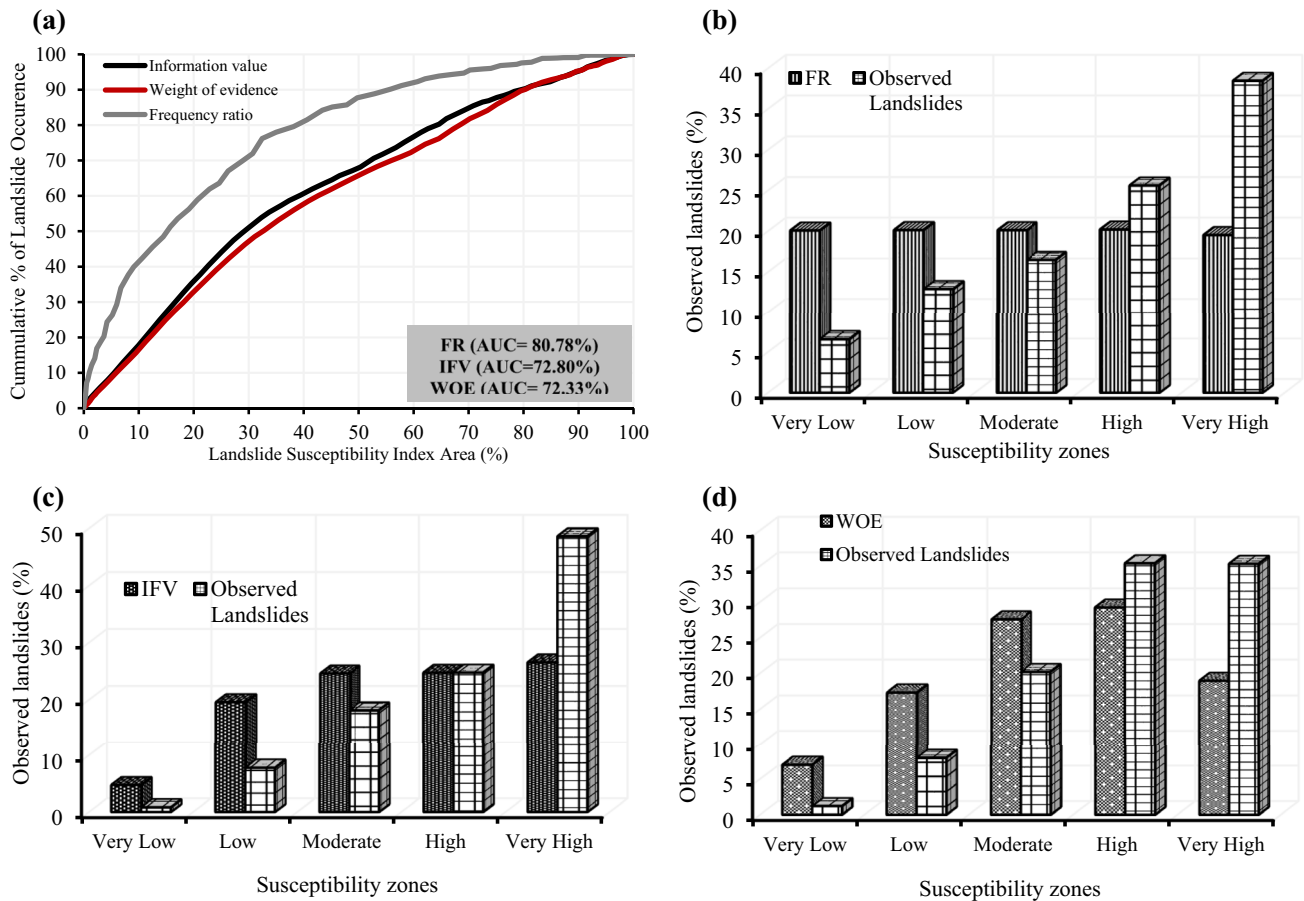


Fig. 7 a Prediction rate curve, b observed landslides in FR susceptibility map, c observed landslides in IFV susceptibility map, d observed landslides in WOE susceptibility map

3.5 Discussion

Figure 6a–c shows the landslide susceptibility maps generated using FR, IFV, and WOE models, respectively, and the relative significance of all influencing factors was evaluated with the occurrence of past landslides and is presented in Fig. 5. In this study, slope angle, elevation, land use/land cover, and roads have high FR, IFV, and W^c , and these factors are considered to be the most significant influencing factors for the occurrence of landslide in the study area which is in agreement with the results obtained by Ozdemir and Altural [21] comparing different models for landslide mapping.

In this study, forest land class from land cover factor has higher W^c , FR, and information value with 0.71, 1.20, and 0.078, respectively, and lower in urban and agriculture land. The observation is in contrast to most of the studies because the forest areas may be more stable. Various studies explained that barren land is more exposed to landslide occurrence due to the direct exposure of climatic factors like, rain, snow, and sun rays [19, 69]; though the case is

Table 1 Landslide distribution in landslide susceptibility zones using SCAI

Methods	Landslide susceptibility zones	% of each zone	% of landslides in each zone	SCAI
FR	Very low	20.06	6.56	2.23
	Low	20.12	12.88	1.13
	Moderate	20.11	16.48	1.36
	High	20.19	25.60	0.79
	Very high	19.50	38.45	0.59
IFV	Very low	4.72	0.80	3.13
	Low	19.56	7.77	1.87
	Moderate	24.54	18.12	1.27
	High	24.67	24.69	1.10
	Very high	26.49	48.59	0.57
WOE	Very low	6.99	1.19	2.22
	Low	17.30	7.977	1.66
	Moderate	27.55	20.16	1.25
	High	29.21	35.37	0.88
	Very high	18.92	35.29	0.61

opposite here, same results have also found in other studies [19, 21, 32, 70]. There could be many reasons behind it, but keeping the condition of the study area in mind, three reasons were found: (1) vegetation cover considered as a significant influencing factor in rainfall-induced landslides [71] and landslides in Thailand triggered due to intensive rainfall [26, 27], (2) the diverse root system of the trees at steep slopes, and (3) weight of the trees and unfavorable wind forces sometimes making the slopes susceptible [72]. The close relationship was found with distance from streams and roads with occurrence of landslides, distance from streams increases the occurrence of landslides decreases and fact found by Yalcin et al. [73] and Ozdemir and Altural [21]; though in roads, the maximum occurrence of landslides is found between 600 and 1500 m, it is because of the natural landslides at higher slopes and elevation. Road cuts are mostly human-induced instability [41].

Similarly, streams can adversely disturb the slope stability by lateral and vertical erosion. Most of the landslides were found in the distance less than 450 m around the streams, and it can be presumed that occurrence of landslide is higher in the vicinity of streams. The slope angle between 2.95° and 68.19° has high tendency to landslide occurrence, and it means that the slope angle increases shear stress in soil as well as in other materials. Flat or gentle slope is less exposed to landslides hazard due to less shear stress associated with the material. The relationship between landslide and slope angle results of this study is in contrast to some previous studies (i.e., [21, 70]) and has consistency with other studies which also elucidated that the occurrence of landslide increases with the increase in angle of slope gradient [20, 50, 51]. Elevation ranging from 177 to 462 m above mean sea level has high trend of landslides, while lower LS trend has found for the elevation ranging from 100–176 to 463–851 m. Occurrence of landslide probability increases with increase in altitude as landslides occur on high slopes. East facing slopes have the higher FR, W^c , and IFV value as compared to other directions and are more susceptible toward landslide (Fig. 5).

To validate the applied models for landslide, mapping success rate curve and prediction rate curve has been applied in this study using the training landslides. The results of success rate curve for FR, IFV, and WOE were 74.60%, 75.04%, and 72.54%, respectively (Fig. 8), while the results of prediction rate for FR, IFV, and WOE were 80.78%, 72.80%, and 72.33%, respectively (Fig. 7a). The accuracy of the applied landslide models was further analyzed using the SCAI technique, and a high number of landslides were found in the higher susceptible zones. Thus, the calculated and classified landslide susceptibility maps are in good agreement. Frequency ratio method showed the highest accuracy in prediction rate curve, but in success rate

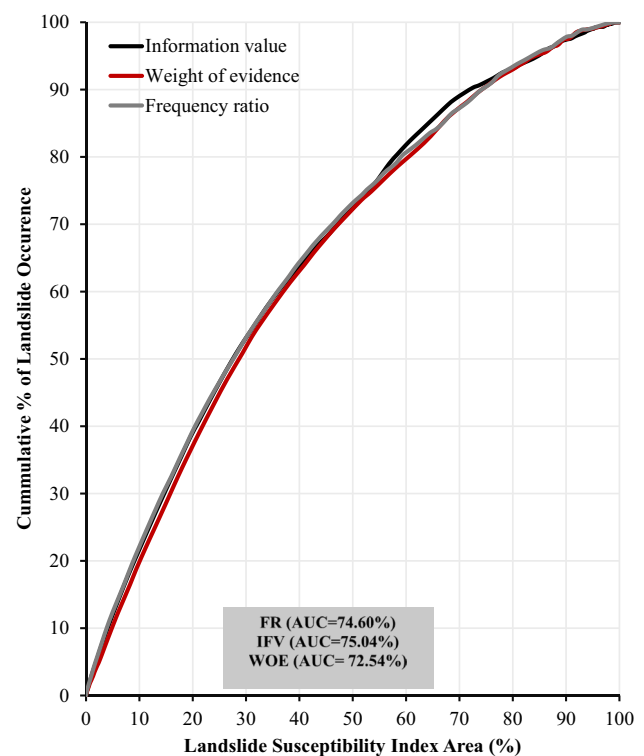


Fig. 8 Success rate curve for landslide susceptibility maps produced from IFV, FR, and WOE methods

curve, the area under curve for all the models was found the same (Fig. 7b–d and Table 1).

The prediction accuracy obtained for frequency ratio in this study is comparable to previous studies [1, 17]. The results of information value method of this study are slightly less than Sarkar et al's. [19] and Chen et al's. [67] study, while it is comparable to Achour et al. [18]. The prediction accuracy for weight of evidence obtained in this study is less than Mathew et al. [20], while it is comparable with the results obtained by Pourghasemi et al. [39]. It is clear from Figs. 7a and 8 that the frequency ratio showed best accuracy in prediction (80.78%) and in success rate curve (74.60%) followed by IFV and WOE.

4 Conclusion

Studies in the past have applied these landslide susceptibility methods, i.e., FR, IR, and WOE, but there lacks an evidence of comparison for selection of most appropriate and accurate technique for the aforementioned study area. Therefore, this study not only utilizes these bivariate approaches but also provides a comparative analysis taking into consideration various influencing factors. Eventually, the results obtained were evaluated via AUC by taking landslide locations in consideration. The accuracy of the

maps was 80.78%, 72.80, and 72.33% for FR, IFV, and WOE, respectively. Upon comparison and evaluation of prediction accuracy among the used quantitative approaches, it was revealed that FR method was highly reliable and accurate. FR method was able to predict almost 80% of the observed landslides as very high, high, and moderate landslide classes. Our results provided the basis to conclude WOE as a complicated method for applying to LS mapping. Several contributing factors for slope failure in Mae Phun include slope gradient, elevation, proximity to roads, and land use/land cover. Conclusively, we ascertain FR method to be most accurate, simple, easy, and intelligible method to be used for LS mapping.

Natural and sometimes human-induced disaster cannot be completely eliminated, but the aftermath can be minimized by proper planning and management. In the study area, there is no meteorological station, and it is suggested that meteorological stations should be installed because landslides in the study area are always associated with rainfall. So, the precipitation is necessary to be integrated with other influencing factors for more accurate results. Indeed, a real-time monitoring module would be more useful for the line department, end-users, and decision makers for a timely emergency response. Landslide susceptibility maps are useful for urban planners and engineers for better development. It can help land use planners with better decision making.

Acknowledgements This work was a part of a Master thesis completed at Naresuan University (Thailand). We are thankful to the department of natural resources and environment for providing the research facilities. We are also thankful to the Land Development Department (LDD) for providing land use data of the study area. Jaruntorn Boonyanuphap and Ghani Rahman reviewed the manuscript many times, and their scientific suggestion has improved the quality of the article. Further, we will extend our acknowledgment to Naresuan University international student scholarship for funding primary author's Master degree.

Compliance with ethical standards

Conflict of interest There is no conflict of interest.

References

- Bourenane H, Guettouche MS, Bouhadad Y, Braham M (2016) Landslide hazard mapping in the Constantine city, Northeast Algeria using frequency ratio, weighting factor, logistic regression, weights of evidence, and analytical hierarchy process methods. *Arab J Geosci* 9(2):154. <https://doi.org/10.1007/s12517-015-2222-8>
- Pradhan B, Mansor S, Pirasteh S, Buchroithner MF (2011) Landslide hazard and risk analyses at a landslide prone catchment area using statistical based geospatial model. *Int J Remote Sens* 32(14):4075–4087. <https://doi.org/10.1080/01431161.2010.484433>
- Yalcin A (2008) GIS-based landslide susceptibility mapping using analytical hierarchy process and bivariate statistics in Ardesen (Turkey): comparisons of results and confirmations. *CATENA* 72(1):1–12. <https://doi.org/10.1016/j.catena.2007.01.003>
- Pradhan B (2011) Manifestation of an advanced fuzzy logic model coupled with Geo-information techniques to landslide susceptibility mapping and their comparison with logistic regression modelling. *Environ Ecol Stat* 18(3):471–493. <https://doi.org/10.1007/s10651-010-0147-7>
- Sarkar S, Kanungo DP, Patra AK, Kumar P (2008) GIS based spatial data analysis for landslide susceptibility mapping. *J Mt Sci* 5(1):52–62. <https://doi.org/10.1007/s11629-008-0052-9>
- Yilmaz I (2009) Landslide susceptibility mapping using frequency ratio, logistic regression, artificial neural networks and their comparison: a case study from Kat landslides (Tokat—Turkey). *Comput Geosci* 35(6):1125–1138. <https://doi.org/10.1016/j.cageo.2008.08.007>
- Lee S, Pradhan B (2007) Landslide hazard mapping at Selangor, Malaysia using frequency ratio and logistic regression models. *Landslides* 4(1):33–41. <https://doi.org/10.1007/s10346-006-0047-y>
- Rahman G, Rahman A, Samiullah, Collins A (2017) Geospatial analysis of landslide susceptibility and zonation in Shahpur valley, Eastern Hindu Kush using frequency ratio model. *Proc Pak Acad Sci* 54(3):149–163
- Feizizadeh B, Blaschke T (2011) Landslide risk assessment based on GIS multi-criteria evaluation: a case study in Bostan-Abad County, Iran. *J Earth Sci Eng* 1(1):66–77
- Rahman G, Rahman A, Ullah S, Miandad M, Collins AE (2019) Spatial analysis of landslide susceptibility using failure rate approach in the Hindu Kush region, Pakistan. *J Earth Syst Sci* 128(3):1–16
- Rai PK, Mohan K, Kumra VK (2014) Landslide hazard and its mapping using remote sensing and GIS. *J Sci Res* 58:1–13
- Sahoo S (2009) A semi quantitative landslide susceptibility assessment using logistic regression model and rock mass classification system. (Masters), ITC, Netherlands. Retrieved from https://www.itc.nl/library/papers_2009/msc/aes/sahoo.pdf
- Corominas J, Van Westen C, Frattini P, Cascini L, Malet JP, Fotopoulou S, Pitilakis K (2014) Recommendations for the quantitative analysis of landslide risk. *Bull Eng Geol Environ* 73:209–263
- Boroumandi M, Khamsehchiyan M, Nikoudel MR (2015) Using of analytic hierarchy process for landslide hazard zonation in Zanjan Province, Iran. In: Lollino G, Giordan D, Crosta GB, Corominas J, Azzam R, Wasowski J, Sciarra N (eds) *Engineering geology for society and territory: landslide processes*, vol 2. Springer, Cham, pp 951–955
- Intarawichian N, Dasananda S (2010) Analytical hierarchy process for landslide susceptibility mapping in lower Mae Chaem watershed, Northern Thailand. *Suranaree J Sci Technol* 17(3):277–292
- Moazzam MFU, Vansarochana A, Boonyanuphap J, Choosumrong S (2017) Landslide assessment using GIS-based frequency ratio method: a case study of Mae-Phun Sub-District, Laplae District, Uttaradit Province, Thailand. Paper presented at the 38th Asian conference on remote sensing, Delhi, India
- Park S, Choi C, Kim B, Kim J (2013) Landslide susceptibility mapping using frequency ratio, analytic hierarchy process, logistic regression, and artificial neural network methods at the Inje area, Korea. *Environ Earth Sci* 68(5):1443–1464. <https://doi.org/10.1007/s12665-012-1842-5>
- Achour Y, Boumezbear A, Hadji R, Chouabbi A, Cavaleiro V, Bendaoud EA (2017) Landslide susceptibility mapping using analytic hierarchy process and information value methods along a highway road section in Constantine, Algeria. *Arab J Geosci* 10(8):194. <https://doi.org/10.1007/s12517-017-2980-6>

19. Sarkar S, Roy A, Martha TR (2013) Landslide susceptibility assessment using information value method in parts of the Darjeeling Himalayas. *J Geol Soc India*. <https://doi.org/10.1007/s12594-013-0162-z>
20. Mathew J, Jha VK, Rawat GS (2007) Weights of evidence modelling for landslide hazard zonation mapping in part of Bhagirathi valley, Uttarakhand. *Curr Sci* 92:628–638
21. Ozdemir A, Altural T (2013) A comparative study of frequency ratio, weights of evidence and logistic regression methods for landslide susceptibility mapping: Sultan Mountains, SW Turkey. *J Asian Earth Sci* 64:180–197. <https://doi.org/10.1016/j.jseae.2012.12.014>
22. Amade N, Painho M, Oliveira T (2018) Geographic information technology usage in developing countries—a case study in Mozambique. *Geo-spatial Inf Sci* 21(4):331–345
23. Greco SE (2018) Seven possible states of geospatial data with respect to map projection and definition: a novel pedagogical device for GIS education. *Geo-spatial Inf Sci* 21(4):288–293
24. Sharma M, Kumar R (2008) GIS based landslide hazard zonation: a case study from the Parwanoo area, lesser and outer Himalaya, H.P., India. *Bull Eng Geol Environ*. <https://doi.org/10.1007/s10064-007-0113-2>
25. Anucharn T (2015) Optimal landslide susceptibility and risk analysis at Khao Phanom Bencha, Krabi Province, Thailand. Ph.D., Suranaree University of Technology
26. Intarawichian N, Dasananda S (2011) Frequency ratio model based landslide susceptibility mapping in lower Mae Chaem watershed, Northern Thailand. *Environ Earth Sci* 64(8):2271–2285. <https://doi.org/10.1007/s12665-011-1055-3>
27. Oh H-J, Lee S, Chotikasathien W, Kim CH, Kwon JH (2008) Predictive landslide susceptibility mapping using spatial information in the Pechabun area of Thailand. *Environ Geol* 57(3):641. <https://doi.org/10.1007/s00254-008-1342-9>
28. Boonyanuphap J (2013) Cost-benefit analysis of vetiver system-based rehabilitation measures for landslide-damaged mountainous agricultural lands in the lower Northern Thailand. *Nat Hazards* 69(1):599–629. <https://doi.org/10.1007/s11069-013-0730-y>
29. Tatong T (2013) The best practices for landslide monitoring and warning in Maephun Subdistrict, Lublue District, Uttaradit Province
30. Ono K, Kazama S, Ekkawatpanit C (2014) Assessment of rainfall-induced shallow landslides in Phetchabun and Krabi provinces, Thailand. *Nat Hazards* 74(3):2089–2107. <https://doi.org/10.1007/s11069-014-1292-3>
31. Phattaraporn S, Anusorn R, Thitawadee S (2017) Analyzing the effects of land use changes for landslide susceptibility assessment: a case study of Lablue District, Uttaradit Province, Thailand. Paper presented at the 38th Asian conference on remote sensing, New Delhi, India
32. Teerarungsigul S, Torizin J, Fuchs M, Kuhn F, Chonglakmani C (2016) An integrative approach for regional landslide susceptibility assessment using weight of evidence method: a case study of Yom River Basin, Phrae Province, Northern Thailand. *Landslides* 13(5):1151–1165. <https://doi.org/10.1007/s10346-015-0659-1>
33. Thammapala P, Weng J (2015) Using geo-informatics for landslide risk map in northern Thailand. Paper presented at the international conference on intelligent earth observing and applications
34. Usamah M, Arambepola N (2013) Lessons learned from the 2006 flashfloods and landslide in Uttaradit and Sukhothai Provinces: implication for effective landslide disaster risk management in Thailand landslide science and practice. Springer, pp 693–699
35. Nachaiboon U, Phewnil O, Duangmal K, Chanwong N, Rollap P, Wichittrakar N, Nimpee C (2014) Effect of landform pattern on soil particles in landslide crisis area of Mae Phun and Mae Phrong Watershed, Uttaradit Province, Northern of Thailand
36. van Westen CJ, Rengers N, Soeters R (2003) Use of geomorphological information in indirect landslide susceptibility assessment. *Nat Hazards* 30(3):399–419. <https://doi.org/10.1023/B:NHAZ.000007097.42735.9e>
37. Ayalew L, Yamagishi H, Ugawa N (2004) Landslide susceptibility mapping using GIS-based weighted linear combination, the case in Tsugawa area of Agano River, Niigata Prefecture, Japan. *Landslides* 1(1):73–81. <https://doi.org/10.1007/s10346-003-0006-9>
38. Guzzetti F, Mondini AC, Cardinali M, Fiorucci F, Santangelo M, Chang K-T (2012) Landslide inventory maps: new tools for an old problem. *Earth-Sci Rev* 112(1–2):42–66. <https://doi.org/10.1016/j.earscirev.2012.02.001>
39. Pourghasemi HR, Pradhan B, Gokceoglu C, Mohammadi M, Moradi HR (2013) Application of weights-of-evidence and certainty factor models and their comparison in landslide susceptibility mapping at Haraz watershed, Iran. *Arab J Geosci* 6(7):2351–2365. <https://doi.org/10.1007/s12517-012-0532-7>
40. Guzzetti F, Carrara A, Cardinali M, Reichenbach P (1999) Landslide hazard evaluation: a review of current techniques and their application in a multi-scale study, Central Italy. *Geomorphology* 31(1):181–216
41. Ayalew L, Yamagishi H, Marui H, Kanno T (2005) Landslides in Sado Island of Japan: Part II. GIS-based susceptibility mapping with comparisons of results from two methods and verifications. *Eng Geol* 81(4):432–445. <https://doi.org/10.1016/j.enggeo.2005.08.004>
42. Magliulo P, Di Lisio A, Russo F, Zelano A (2008) Geomorphology and landslide susceptibility assessment using GIS and bivariate statistics: a case study in southern Italy. *Nat Hazards* 47(3):411–435. <https://doi.org/10.1007/s11069-008-9230-x>
43. Akgun A, Türk N (2010) Landslide susceptibility mapping for Ayvalik (Western Turkey) and its vicinity by multicriteria decision analysis. *Environ Earth Sci* 61(3):595–611. <https://doi.org/10.1007/s12665-009-0373-1>
44. Balamurugan G, Ramesh V, Touthang M (2016) Landslide susceptibility zonation mapping using frequency ratio and fuzzy gamma operator models in part of NH-39, Manipur, India. *Nat Hazards* 84(1):465–488. <https://doi.org/10.1007/s11069-016-2434-6>
45. Çevik E, Topal T (2003) GIS-based landslide susceptibility mapping for a problematic segment of the natural gas pipeline, Hendek (Turkey). *Environ Geol* 44(8):949–962. <https://doi.org/10.1007/s00254-003-0838-6>
46. Jaiswal P, van Westen CJ, Jetten V (2010) Quantitative landslide hazard assessment along a transportation corridor in southern India. *Eng Geol* 116(3):236–250. <https://doi.org/10.1016/j.enggeo.2010.09.005>
47. Deniz T, Paletto A (2018) Effects of bioenergy production on environmental sustainability: a preliminary study based on expert opinions in Italy and Turkey. *J For Res* 29(6):1611–1626
48. Dai FC, Lee CF, Li J, Xu ZW (2001) Assessment of landslide susceptibility on the natural terrain of Lantau Island, Hong Kong. *Environ Geol* 40(3):381–391. <https://doi.org/10.1007/s002540000163>
49. Saha AK, Gupta RP, Arora MK (2002) GIS-based Landslide Hazard Zonation in the Bhagirathi (Ganga) Valley, Himalayas. *Int J Remote Sens* 23(2):357–369. <https://doi.org/10.1080/0143160010014260>
50. Dahal RK, Hasegawa S, Nonomura A, Yamanaka M, Dhakal S, Paudyal P (2008) Predictive modelling of rainfall-induced landslide hazard in the Lesser Himalaya of Nepal based on weights-of-evidence. *Geomorphology* 102(3–4):496–510. <https://doi.org/10.1016/j.geomorph.2008.05.041>

51. Dahal RK, Hasegawa S, Nonomura A, Yamanaka M, Masuda T, Nishino K (2008) GIS-based weights-of-evidence modelling of rainfall-induced landslides in small catchments for landslide susceptibility mapping. *Environ Geol* 54(2):311–324. <https://doi.org/10.1007/s00254-007-0818-3>
52. Demir G, Aytekin M, Akgün A, İkizler SB, Tatar O (2013) A comparison of landslide susceptibility mapping of the eastern part of the North Anatolian Fault Zone (Turkey) by likelihood-frequency ratio and analytic hierarchy process methods. *Nat Hazards* 65(3):1481–1506. <https://doi.org/10.1007/s11069-012-0418-8>
53. Kavzoglu T, Sahin EK, Colkesen I (2014) Landslide susceptibility mapping using GIS-based multi-criteria decision analysis, support vector machines, and logistic regression. *Landslides* 11(3):425–439. <https://doi.org/10.1007/s10346-013-0391-7>
54. Kayastha P, Dhital MR, De Smedt F (2013) Application of the analytical hierarchy process (AHP) for landslide susceptibility mapping: a case study from the Tinau watershed, west Nepal. *Comput Geosci* 52:398–408. <https://doi.org/10.1016/j.cageo.2012.11.003>
55. Lee S, Ryu JH, Min K, Won JS (2003) Landslide susceptibility analysis using GIS and artificial neural network. *Earth Surf Process Landf* 28(12):1361–1376. <https://doi.org/10.1002/esp.593>
56. Pradhan B (2010) Application of an advanced fuzzy logic model for landslide susceptibility analysis. *Int J Comput Intell Syst.* <https://doi.org/10.1080/18756891.2010.9727707>
57. Moore ID, Grayson RB, Ladson AR (1991) Digital terrain modeling: a review of hydrological, geomorphological, and biological applications. *Hydrol Process* 5(1):3–30. <https://doi.org/10.1002/hyp.3360050103>
58. Kanwal S, Atif S, Shafiq M (2016) GIS based landslide susceptibility mapping of northern areas of Pakistan, a case study of Shigar and Shyok Basins. *Geomat Nat Hazards Risk.* <https://doi.org/10.1080/19475705.2016.1220023>
59. Lee S, Min K (2001) Statistical analysis of landslide susceptibility at Yongin, Korea. *Environ Geol* 40(9):1095–1113. <https://doi.org/10.1007/s002540100310>
60. Oh H-J, Kim Y-S, Choi J-K, Park E, Lee S (2011) GIS mapping of regional probabilistic groundwater potential in the area of Pohang City, Korea. *J Hydrol* 399(3):158–172. <https://doi.org/10.1016/j.jhydrol.2010.12.027>
61. Yin K, Yan T (1988) Statistical prediction model for slope instability of metamorphosed rocks. Paper presented at the Proceedings of the 5th international symposium on landslides
62. van Westen CJ (1993) Application of geographic information systems to landslide hazard zonation. International Institute for Geo-Information Science and Earth Observation, Enschede
63. Vansarochana A, Tripathi NK, Clemente R (2009) Investigating mudslide phenomenon in Mae Cham Basin, Thailand. Paper presented at the geoinformation technology for natural disaster management and rehabilitation, Bangkok, Thailand
64. Zêzere JL (2002) Landslide susceptibility assessment considering landslide typology. A case study in the area north of Lisbon (Portugal). *Nat Hazards Earth Syst Sci* 2(1/2):73–82
65. Saha AK, Gupta RP, Sarkar I, Arora MK, Csaplovics E (2005) An approach for GIS-based statistical landslide susceptibility zonation—with a case study in the Himalayas. *Landslides* 2(1):61–69. <https://doi.org/10.1007/s10346-004-0039-8>
66. Bonham-Carter GF (1989) Weights of evidence modeling: a new approach to mapping mineral potential. *Stat Appl Earth Sci* 98:171–183
67. Chen T, Niu RQ, Jia XP (2016) A comparison of information value and logistic regression models in landslide susceptibility mapping by using GIS. *Environ Earth Sci* 75(10):867. <https://doi.org/10.1007/s12665-016-5317-y>
68. Süzen ML, Doyuran V (2004) A comparison of the GIS based landslide susceptibility assessment methods: multivariate versus bivariate. *Environ Geol* 45(5):665–679. <https://doi.org/10.1007/s00254-003-0917-8>
69. Bacha AS, Shafique M, van der Werff H (2018) Landslide inventory and susceptibility modelling using geospatial tools, in Hunza-Nagar valley, northern Pakistan. *J Mt Sci* 2018:1–17
70. Mohammady M, Pourghasemi HR, Pradhan B (2012) Landslide susceptibility mapping at Golestan Province, Iran: a comparison between frequency ratio, Dempster–Shafer, and weights-of-evidence models. *J Asian Earth Sci* 61:221–236. <https://doi.org/10.1016/j.jseae.2012.10.005>
71. Begueria S (2006) Changes in land cover and shallow landslide activity: a case study in the Spanish Pyrenees. *Geomorphology* 74(1):196–206. <https://doi.org/10.1016/j.geomorph.2005.07.018>
72. Green-way DR (1987) Vegetation and slope stability. In: Anderson MG, Richards KS (eds) *Slope stability*. Wiley, Chichester, pp 187–230
73. Yalcin A, Reis S, Aydinoglu AC, Yomralioglu T (2011) A GIS-based comparative study of frequency ratio, analytical hierarchy process, bivariate statistics and logistics regression methods for landslide susceptibility mapping in Trabzon, NE Turkey. *CATENA* 85(3):274–287. <https://doi.org/10.1016/j.catena.2011.01.014>

Publisher's Note Springer Nature remains neutral with regard to jurisdictional claims in published maps and institutional affiliations.